


## ORIGINAL ARTICLE

# Piepkorn type of osteochondrodysplasia: Defining the severe end of *FLNB*-related skeletal disorders in three fetuses and a 106-year-old exhibit

Helga Rehder<sup>1,2\*</sup>  | Franco Laccone<sup>1\*</sup> | Susanne G. Kircher<sup>1</sup> | Ralf L. Schild<sup>3</sup> |  
 Christiane Rapp<sup>4</sup> | Rainer Bald<sup>5</sup> | Bernt Schulze<sup>6</sup> | Jana Behunova<sup>1</sup> |  
 Juergen Neesen<sup>1</sup> | Katharina Schoner<sup>2</sup>

<sup>1</sup>Institute of Medical Genetics, Medical University of Vienna, Vienna, Austria

<sup>2</sup>Institute of Pathology, Philipps University of Marburg, Marburg, Germany

<sup>3</sup>Department of Obstetrics, Diacovere Friederikenstift, Hannover, Germany

<sup>4</sup>Department of Praenatal Medicine, Klinikum Oldenburg, Oldenburg, Germany

<sup>5</sup>Clinic of Gynaecology and Obstetrics, Klinikum Leverkusen, Leverkusen, Germany

<sup>6</sup>Practice for Human Genetics, Hannover, Germany

## Correspondence

Helga Rehder, Institute of Medical Genetics, Medical University of Vienna, Waehringer Strasse 10, Vienna A-1090, Austria.

Email: helga.rehder@meduniwien.ac.at

The Piepkorn type of lethal osteochondrodysplasia (POCD) is a rare and lethal dwarfing condition. Four cases have been reported to date. The characteristic features are distinctly shortened “flipper-like” limbs, polysyndactyly, excessive underossification, especially of the limb bones and vertebrae, and large (giant) chondrocytes in the cartilaginous bone primordia. These characteristics allowed the diagnosis of Piepkorn type of osteochondrodysplasia in four new cases, three fetuses of 15 to 22 weeks and one 106-year-old museum exhibit. Piepkorn type of osteochondrodysplasia has been assigned to the giant cell chondrodysplasias such as atelosteogenesis type 1 (AO1) and boomerang dysplasia (BD). Analysis of the *Filamin B* gene in 3p14.3, which is associated with these disorders, allowed the identification of the first *FLNB* mutations in Piepkorn type of osteochondrodysplasia. The heterozygous missense mutations, found in the three fetuses, were located in exons 28 and 29, encoding the immunoglobulin-like repeat region R15, one of three mutational hot spots in dominant *FLNB*-related skeletal disorders. Direct preparations and alcian blue staining revealed single upper and lower arm and leg bone primordia, preaxial oligodactyly, and polysyndactyly with complete fusion and doubling of the middle and end phalanges II–V to produce eight distal finger rays. Considering the unique clinical features and the extent of underossification, Piepkorn type of osteochondrodysplasia can be regarded as a distinct entity within the AO1-BD-POCD continuum.

## KEYWORDS

atelosteogenesis type 1, boomerang dysplasia, fetal skeletal dysplasias, *FLNB*, Piepkorn type of osteochondrodysplasia, XY sex reversal

## 1 | INTRODUCTION

In 1977, Piepkorn et al. described a case of lethal neonatal dwarfism that they thought was “unique in the severity of trunk-limb disproportion, the symphalangism of the hands and the lack of recognizable ossification in the limbs.” This condition, later named “Piepkorn syndrome” or “Piepkorn type of lethal osteochondrodysplasia” (POCD), is not well recognized as a separate entity in many major textbooks and online databases. Only four cases have been documented to date, one representing a 100-year-old anatomical specimen of the Museum Vrolik collection in Amsterdam (Canki-Klain et al., 1992; Oostra, Dijkstra, Baljet,

Verbeeten, & Hennekam, 1999; Piepkorn, Karp, Hickok, Wiegenstein, & Hall, 1977; Urioste et al., 1997). The classical features are severe underossification of the skeleton associated with extremely short flipper-like limbs, short ribs, polysyndactyly, craniosynostosis, and a characteristic facies with a bulging forehead, widely spaced protruding eyes, a very short, flat and upturned nose, microstomia, Pierre Robin anomaly, and posteriorly rotated, low-set ears. Hydrops, omphalocele, polyhydramnios, and malformations of the central nervous, cardiovascular, and urogenital system have also been observed. Piepkorn type of osteochondrodysplasia was initially regarded as a new variety of “short-rib polydactyly dwarfism” (Piepkorn et al., 1977). With respect to the characteristic bone histology, namely, the presence of large or giant chondrocytes, so far observed in atelosteogenesis type 1 (AO1)

\*These authors contributed equally to this work.

The copyright line of this article has been corrected after the original publication 23 May 2018

This is an open access article under the terms of the Creative Commons Attribution NonCommercial License, which permits use, distribution and reproduction in any medium, provided the original work is properly cited and is not used for commercial purposes

and boomerang dysplasia (BD), POCD has been assigned to the category of giant cell chondrodysplasias (AO-BD-POCD spectrum) (Oostra et al., 1999) or, as the "Piepkorn type of BD (Canki-Klain et al., 1992; Superti-Furga, Unger, & Nosology Group of the International Skeletal Dysplasia Society, 2007; Urioste et al., 1997) or of type 1 atelosteogenesis" (Warman et al., 2011), was thought to represent a severe manifestation of these disorders.

Heterozygous mutations in the *filamin B* gene (*FLNB*, MIM \*603381) in 3p14.3, cause dominant BD (MIM #112310), atelosteogenesis 1 and 3 (MIM #108720 and #108721), Larsen syndrome (LS) (MIM #150250), seemingly isolated congenital talipes equinovarus and recessive spondylcarpotarsal synostosis (MIM # 272460) (Bicknell et al., 2005; Daniel et al., 2012, Yang et al., 2016; Krakow et al., 2004).

Filamins are intracytoplasmic actin-binding proteins that regulate the structure and activity of the cytoskeleton by crosslinking F-actin fibrils into a membrane-bound three-dimensional cytoskeletal network. As a leading scaffold for intracellular signaling and protein trafficking pathways, it also interacts with intracellular proteins and thereby regulates cytoskeleton-dependent cell proliferation and differentiation (Cunningham et al., 1992; Krakow et al., 2004; Nakamura et al., 2011; Stossel et al., 2001; Van der Flier & Sonnenberg, 2001). *FLNB* is strongly expressed in epiphyseal growth plate chondrocytes and developing vertebral bodies. It contains an N-terminal actin-binding domain (ABD) with two calponin homology subdomains CH1 and CH2, followed by 24 immunoglobulin-like tandem repeats (R1–24) and two flexible hinge regions: hinge 1 between R15 and 16 and hinge 2 between R23 and 24 (Chakarova et al., 2000). Mutations are thought to disrupt enchondral ossification by a yet unknown mechanism. The ABD and the *FLNB* repeat regions R14 and R15 represent mutational hot spots for the dominant *FLNB*-related skeletal disorders.

We present three fetuses and a 106-year-old formalin-fixed exhibit with the Piepkorn type of osteochondrodysplasia and the first *FLNB* mutations reported in association with this condition.

## 2 | MATERIALS AND METHODS

Fetal Cases 1–3 are from the "Fetal Pathology Working Group" at the Institute of Pathology in Marburg, where they were sent from obstetric departments in Germany (Hannover, Oldenburg, and Leverkusen). The fetal autopsies included X-rays, alcian blue cartilage staining of the limbs, histology, and photographic documentations (for details, see Schoner et al., 2017; and the Supporting Information on modified alcian blue dyeing technique). Case 4 is an exhibit from the pathoanatomical collection ("Fool's Tower collection") of the Museum of Natural History in Vienna. The body had been stored in 10% formaldehyde since 1910 and in a solution of ethanol:glycerin:distilled water (volume 2:3:5) for the past 2 years. Autopsy had not been performed. Recent radiological investigations included a three-dimensional reconstruction of the skeleton based on whole-body computer tomography. Skin biopsies were taken for paraffin embedding.

Fetograms of two male fetuses, one with BD at 35 weeks (Kozłowski, Tsuruta, Kameda, Kan, & Leslie, 1981) and one with type 1

atelosteogenesis at 16 + 2 weeks (own observation) were used to compare radiographic changes with other severe *FLNB*-related chondrodysplasias (see Table 1 and attached Figure 5a–c).

For molecular analyses, informed consent was obtained from the parents. For Case 4, the consent of the Ethics Committee of the Medical University of Vienna was obtained. The tests had been performed at the Institute of Medical Genetics in Vienna. Genomic DNA was extracted from parental blood and from frozen samples of the fetal tissues (skeletal muscle, skin) according to standard procedures using the DNeasy Blood & Tissue Kit (Qiagen, Vienna, Austria). DNA from the museum case was extracted after the paraffin embedding of skin probes using the QIAamp DNA FFPE Tissue Kit. The 46 coding exons and adjacent intronic sequences of the *FLNB* gene were amplified by polymerase chain reaction (PCR) and then underwent Sanger sequencing. Sequence analyses were done on a 3500 Genetic Analyzer (Life Technologies) using the sequence pilot software analysis tool (JSI medical systems). Primer sequences used for PCR and sequence analyses can be provided on request. The same procedure was applied to analyze the *SOX9* (MIM \*608160), *SF1* (MIM \*601516), *DHH* (MIM \*605432), and *CBX2* (MIM \*602770) genes in Case 3. *DAX1* (MIM \*300473) and the *SRY* (MIM \*480000) region were investigated by fluorescence in situ hybridization and array comparative genomic hybridization.

## 3 | RESULTS

### 3.1 | Clinical reports

Fetus 1 was the second conceptus of a 38-year-old woman and her 52-year-old husband, both with mild intellectual disabilities, the mother because of reported perinatal hypoxia (see Table 1). The unrelated couple was of German origin. The family history was uneventful. A first pregnancy had been terminated for unknown reasons. Prenatal ultrasound during the second pregnancy, performed at 21 + 3 weeks of gestation, identified a hydropic fetus with tetraphocomelia and abnormal facies (Figure 1a). The fetal karyotype was normal, 46,XX. The pregnancy was terminated at 21 + 5 weeks. No information could be obtained about any further pregnancies.

Fetus 2 was the third conceptus of a 42-year-old gravida III/para I and her nonconsanguineous 46-year-old husband (see Table 1). The couple is of German descent. The family history was uneventful. The firstborn son is healthy. The second pregnancy ended in an early miscarriage. Prenatal ultrasound at 13 + 4 and 15 + 5 weeks of gestation of the third pregnancy revealed fetal hydrops, hygroma colli, and lacking limbs with hands and feet, almost attached to the trunk (Figure 1b). The chromosomes were normal, 46,XX. The pregnancy was terminated at 15 + 6 weeks. There were no subsequent pregnancies.

Fetus 3 was the first conceptus of a 36-year-old woman and her unrelated, 46-year-old husband, both of German origin (see Table 1). The pregnancy had been complicated by a maternal parvovirus B19 infection. Prenatal ultrasound at 15 + 0 weeks of gestation revealed fetal hydrops, excessive shortening of the limbs, and underossification of the vertebrae, leading to the tentative diagnosis of achondrogenesis (Figure 1c). The pregnancy was terminated at 16 weeks. The fetus was

TABLE 1 Clinical data

Features	Case 1	Case 2	Case 3	Case 4 exhibit <sup>a</sup>	AO1 case	BD case (Kozlowski et al., 1981)
Maternal age	38	42	36	?	29	29
Para/gravida	0/2	1/3	0/1	?	0/1	1/1
Gestational week	21 + 5	15 + 6	16th	32th (estimated)	16 + 2	35
Weight/length	264 g/17 cm	45 g/8.5 cm	30 g/7.5 cm	800 g/21.5 cm	99 g/14.5 cm	1850 g/32 cm
Karyotype/genitals	46,XX/♀	46,XX/♀	46,XY/♀	N.d./♀	46,XY/♂	N.d./♂
FLNB mutation	Exon 29 c.5094C>A p. Ser1698Arg	Exon 29 c.5095C>A p. Pro1699Thr	Exon 28 c.4850G>A p. Cys1617Tyr	N.d.	Exon 3 c.626T>A p. Leu209Gln	N.d.
Hydrops/hygroma colli	+/+	+/+	+/+	+/+	+ / (+)	+ / -
Polyhydramnios	-	-	-	N.d.	-	+
Cran.-fac. features:						
Macrobrachycephaly	+	+	+	+	+	+
Wide sutures	+	+	+	+	+	?
Bulging forehead	+	+	+	+	+	+
Hypertelorism	++	+	+	+	+	?
Exophthalmos	++	+	+	+	-	-
Microstomia	+	+	+	+	+	-
Microretrognathia	+	+	+	+	+	+
Pierre Robin anomaly	+	+	+	CLP bilat.	+	?
Ear anomalies	+	+	+	+	+	+
Micromelic dwarfism	+	+	+	+	+	+
Flipper-like limbs	+	+	+	+	-	-
Oligo-/poly-/syndact. fingers	+ / 8 / +	+ / 8 / +	(+) / 8 / +	? / N.d. / +	-	-
Oligo-/poly-syndact.	+ / + / +	+ / ? / +	+ / + / +	? / ? / +	-	+ / - / -
Nubbin-like digits	+	+	+	+	BrD + SpT	BrD
X-ray of						
Humeri	AO	AO	AO	AO <sup>b</sup>	AO	AO
Ulnae	AO	AO	AO	AO <sup>b</sup>	Short	Triangular
Radii	AO	AO	AO	AO <sup>b</sup>	Short	Triangular
Femora	AO	AO	AO	AO <sup>b</sup>	UO	AO
SFLB	AO	AO	AO	AO <sup>b</sup>	O	O - angulated
Vertebral bodies	AO	AO	AO	AO <sup>b</sup>	AO (partial)	UO
Ribs	AO	UO	AO	UO <sup>b</sup>		-
Clavicles	UO (short)	UO (short)	UO (short)	UO <sup>b</sup> (short)	O	Hooked
Scapulae	UO	UO	UO	UO <sup>b</sup>	Hooked	UO
Iliac bones	AO	UO	AO	AO <sup>b</sup>	UO	UO
Pubic bones	AO	UO	AO	AO <sup>b</sup>	UO	AO
Metacarpals	AO	AO	AO	AO <sup>b</sup>	AO	AO

(Continues)

TABLE 1 (Continued)

Features	Case 1	Case 2	Case 3	Case 4 exhibit <sup>a</sup>	AO1 case	BD case (Kozłowski et al., 1981)
Metatarsals	AO	AO	AO	AO <sup>b</sup>	AO	?
Skull/skull base	UO/ossified	UO/ossified	UO/ossified	UO <sup>b</sup> /ossified	AO UO/O	?
Bone cartilage histology/multinucleated giant cells	LCh+VCh/ (+)	LCh+VCh/–	LCh+VCh/–	N.d.	LCh+VCh/+	VCh/?
Prominent abdomen	+	+	+	+	+	+
Omphalocele	–	+	–	+	–	–
Cardiac defect	ASD II	–	+	N.d.	ASD II	?
Urogenital anomalies	KU, BU, HG	BU	Sex reversal with ovaries	N.d.	–	?
Miscellaneous	LH, MC, EA, PI	LH, MC, EA	LH, MC, parvovir. B19	N.d.	LH	?

AO = absent ossification; ASD = atrial septal defect; BD = boomerang dysplasia; BrD = brachydactyly; BU = bicornuate uterus; C(L)P = cleft (lip and) palate; EA = ectopic anus; HG = hypoplastic genitalia; KU = kinky ureters; LCh = large chondrocytes; LH = lung hypoplasia; MC = mobile coecum; O = ossified; PI = premature incisors; SFLB = single foreleg bone; UO = underossification; VCh = vacuolated chondrocytes; N.d. = not determined.

<sup>a</sup>Formalin fixed >100 years yellow (no) shade marks the POCD cases; Pink (grey) shade marks the AO1 and BD cases.

<sup>b</sup>Three-dimensional reconstruction on whole-body computed tomography (Case 4).

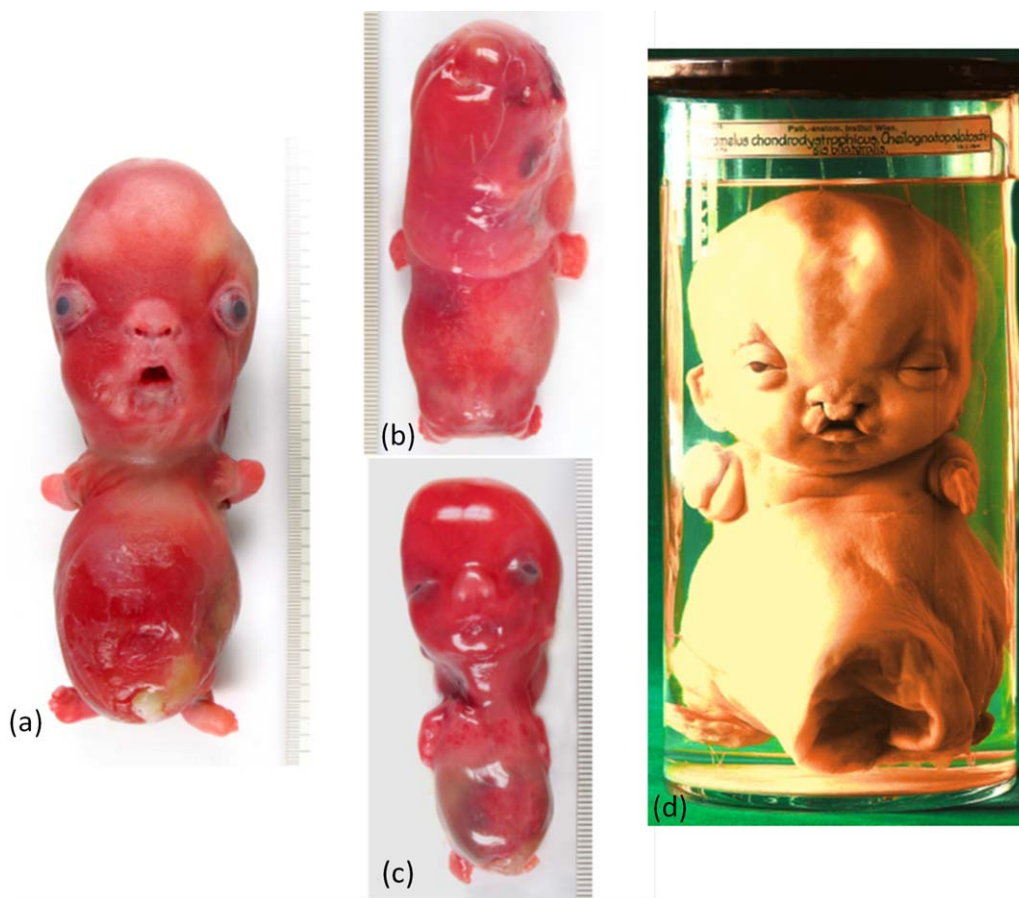
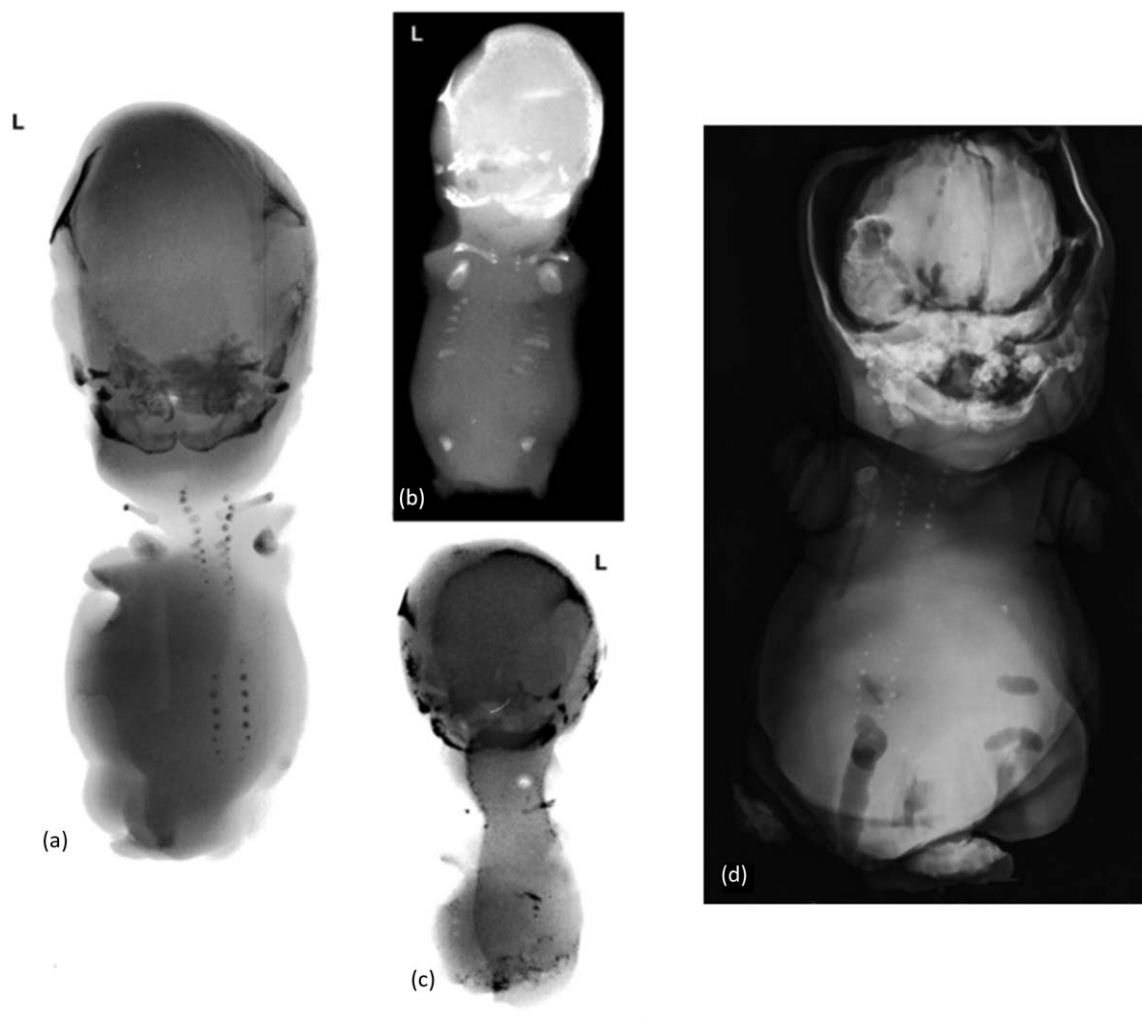


FIGURE 1 Frontal and dorsal aspect of four fetuses with POCD showing hydrops with cystic hygroma, short flipper-like limbs, protuberant abdomen with or without omphalocele, large skull, wide sutures and dysmorphic facies. (a) Case 1, female (XX), 21 + 5 weeks; (b) Case 2, dorsal view, female (XX), 15 + 6 weeks; (c) Case 3, female phenotype (XY), 16 weeks; (d) Case 4, 106-year-old museum exhibit, female neonate (photo of case 4 from Hauser, 1998)



**FIGURE 2** Radiographs in posterior-anterior-/anterior-posterior—(PA-/AP- projection: a,b,d,c) showing absent ossification of the limb bones and vertebral bodies and deficient ossification of the ribs, clavicles, scapulae, pelvic bones, and skull with partial coronal craniosynostosis. Well-ossified: vertebral pedicles, cranial base and lower facial bones. (a) Case 1, female, 21 + 5 weeks; (b) Case 2, female, 15 + 6 weeks; (c) Case 3, female phenotype (46,XY), 16 weeks; (d) Case 4, 106-year-old exhibit, female neonate. L = left side

phenotypically female. Postnatal chromosome analysis on the fetal fibroblasts revealed 46,XY karyotype. Two subsequent pregnancies produced a normal boy and girl with normal karyotypes.

Fetus 4, the exhibit in the pathoanatomical Fool's Tower collection in Vienna, was diagnosed by us with Piepkorn syndrome. No information on the origin and clinical data of this 106-year-old exhibit was available (Figure 1d). Gestational age was estimated as 32 weeks (see Table 1).

### 3.2 | Autopsy

The three fetuses in Cases 1–3 weighed 264, 45, and 30 g and had crown-rump lengths of 14.5, 7.5, and 7 cm and crown-heel lengths of 17, 8.5, and 7.5 cm, respectively. The fixed museum specimen in Case 4 was 800 g in weight and 21.5 cm in length. All four cases were phenotypically female, in Case 3 due to XY sex reversal. They displayed severe hydrops with large nuchal blebs (Figure 1b) and micromelic dwarfism with extremely short flipper-like limbs, brachydactyly and complete syndactyly of all fingers and toes, short trunk, and macrocephaly with an extremely wide anterior fontanel and wide sagittal and frontal sutures

(Figures 1a–d and 2a–d). The facies showed a high and bulging forehead, shallow orbits, pronounced hypertelorism, and prominent (and in Case 1 protruding) laterally set eyes. A short flat nose, microstomia, and microretrognathia were noted, resulting in a Pierre Robin anomaly in Cases 1–3, while Case 4 had a bilateral cleft lip and palate. The ears were low set and posteriorly rotated, the neck was short, the thorax was short and narrow, and the lungs were accordingly hypoplastic. The abdomen was distended and associated with an omphalocele in Cases 2 & 4. No major internal anomalies were observed. Parvo B19 viral inclusions were found in the liver, kidneys, and placenta of Case 3 by immunohistochemistry. Despite a 46,XY karyotype, the fetus in Case 3 presented with female external and internal genitalia and ovaries and thus showed true sex reversal. Direct preparation allowed the identification of a single cartilage anlage in the upper and lower arms and legs. These bone models were short and thick but straight, separated by a narrow slit without regular joint formation. The cartilage anlagen in the legs were in an acute angular position (Figure 3h = Case 1).

No autopsy was performed on the exhibit.

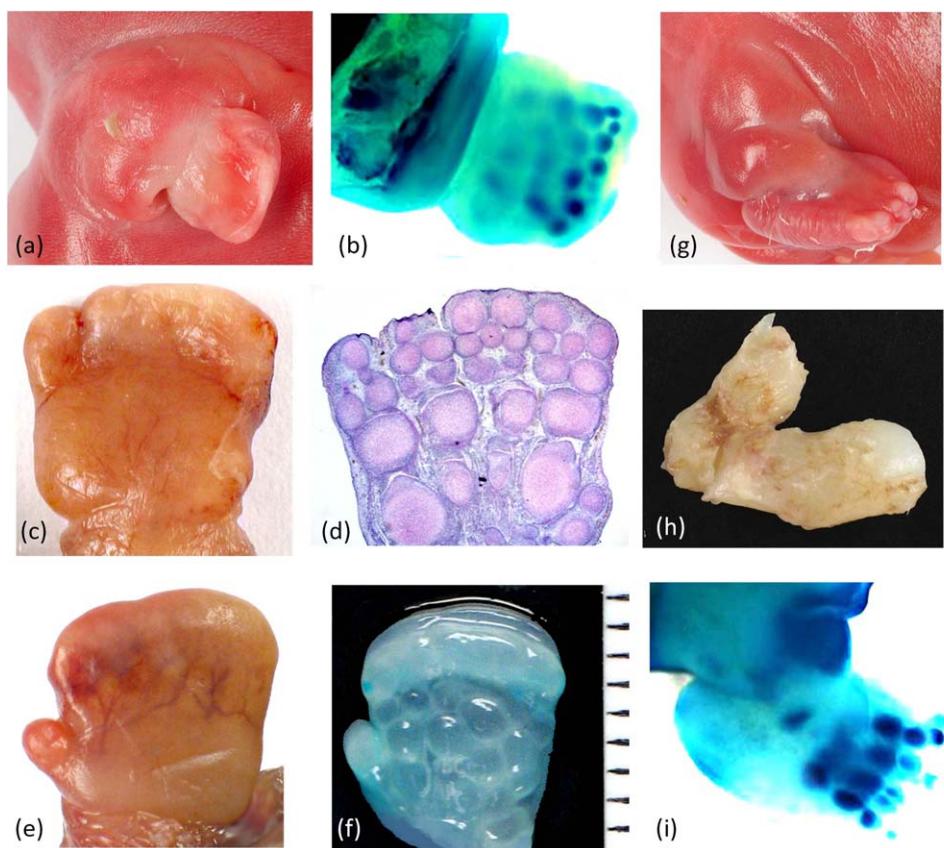


**FIGURE 3** Hands and foot of Case 1 (a,b,g–i), Case 2 (c,d), and Case 3 (e,f) displaying complete syndactyly of fingers, missing or hypoplastic thumb and hallux, and, via alcian blue staining for fetal cartilage (b,f,i) and histology (d), Periodic acid-Schiff reaction (PASx1,25) duplication of the distal finger rays, resulting in distal octodactyly. There is also horizontal segmentation of the metacarpals and metatarsals. Direct preparation of the lower limb (h) shows single cartilage anlagen of the upper and the lower leg in an angular boomerang-like position

### 3.3 | Radiological findings

X-ray examination showed an almost identical lack of ossification in the limb bones, ribs, and vertebrae, excluding the lateral pedicles in Cases 1, 2, and 4. Underossification of the skull, excluding the skull base and lower facial bones, a wide sagittal and frontal suture, and partially craniosynostotic coronal sutures were observed. The clavicles were short, and the scapulae and iliac bones were small. However, the cases differed slightly in that there were partially ossified ribs and an additional lack of ossification in most of the lateral pedicles in Case 2 (Figure 2a–d).

### 3.4 | Alcian blue cartilage staining

Alcian blue staining of the right hand and foot (Cases 1 + 3) and histological sections of the right hand and foot (Cases 2 + 3) identified two single straight and short upper and lower limb cartilages, preaxial oligodactyly of the hands and feet with either missing (Case 1 + 2) or short thumbs (Case 3) and four short metacarpals/metatarsals plus a rudimentary first metacarpal/metatarsal. Doubling of the middle and end phalanges of digits II–V produced eight distal finger rays. The phalanges were distinctly shortened, and the metacarpals/metatarsals were

horizontally split and the segments round in shape. The syndactyly appeared to be purely cutaneous (Figure 3a–i).

### 3.5 | Histological findings

The hyaline cartilages from the right lower limb (Cases 1–3) and the right hand (Case 2) showed no endochondral or perichondrial ossification or mineralization. There were monomorphic, evenly distributed chondrocytes with high cellularity in the peripheral parts (Figure 4a), while in more central parts of the cartilage anlagen the distribution of chondrocytes was irregular, with hypocellular or acellular areas of homogeneous amorphous extracellular matrix. Higher magnifications identified variations in the cellular and nuclear size and moderate pleomorphism. The cells displayed prominent nuclei, perinuclear cytoplasmic retraction and vacuolization, and circumferential halos (Figure 4b,c). No mitoses were identified. One larger cell was almost classifiable as a giant cell (Figure 4c). True multinucleated stellate giant chondrocytes were found in our AO1 case with the CH2 mutation (Figure 4d).

### 3.6 | *FLNB* gene molecular analysis

In the three analyzed fetuses a heterozygous mutation was detected in the *FLNB* gene. All identified variations resulted in missense mutations.

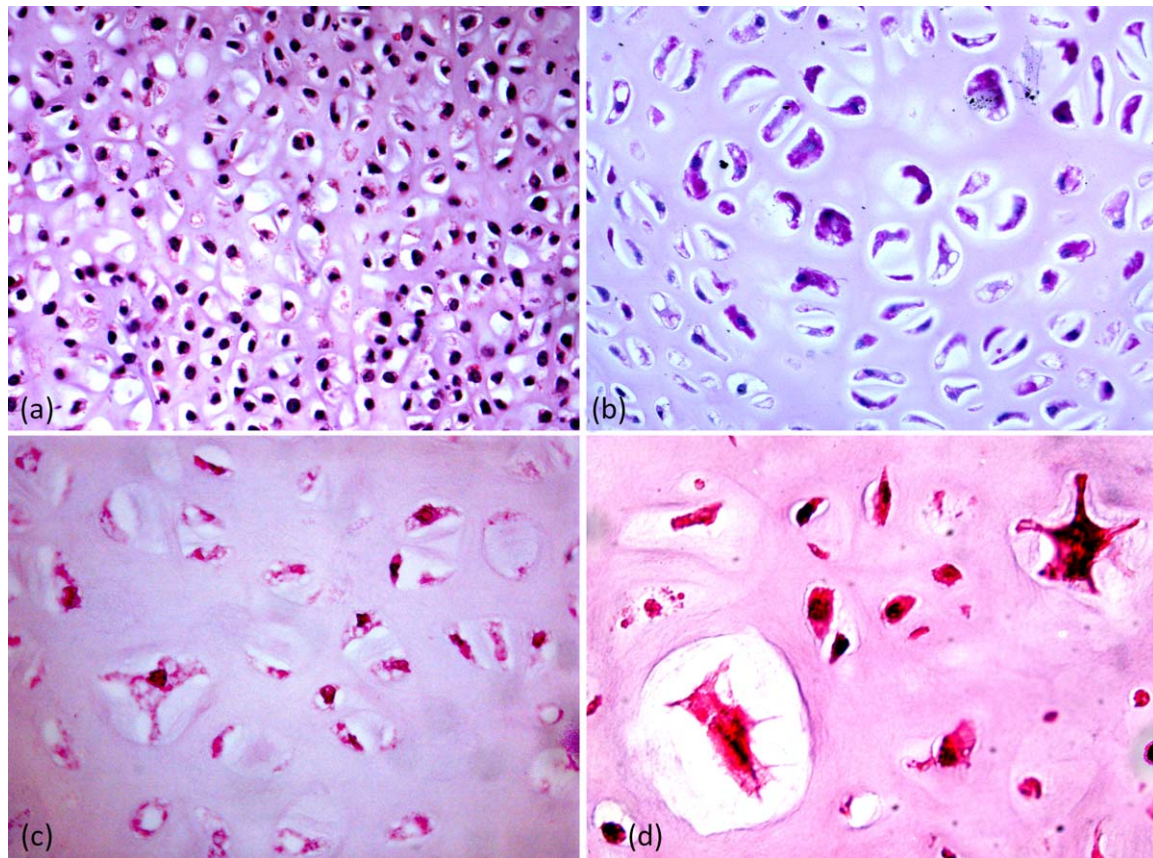


**FIGURE 4** Histology of cartilage anlagen shows densely packed smaller chondrocytes in peripheral parts (a), irregular distribution of pleomorphic, partly binucleated or multinucleated and large chondrocytes in more central parts with retracted vacuolized cytoplasm, surrounding halos (b–d), a single giant cell-like stellate chondrocyte (c) and multiple true multinucleated giant cells (d). (a) Case 3, right leg bone, HEx40; (b) Case 2, right metacarpal bone, PASx40; (c) Case 1, right leg bone, HEx63; (d) AO1 case, male, 16 + 2 weeks, left femur, HEx63

The variations c.5094C > A [p.(Ser1698Arg), Case 1], c.5095C > A [p.(Pro1699Thr), Case 2], and c.4850G > A [p.(Cys1617Tyr), Case 3] were located in exons 28 and 29, respectively, encoding the last repeat 15 of filamin B repeat domain 1 (rod 1). In Case 4, the quality of the DNA extracted from the histological slides was not sufficient for the amplification and sequencing of the gene. A fourth identified variation [c.626T > A, p.(Leu209Gln)], detected in our AO1-case affected the calponin homology domain 2 of filamin B. All variants seem to have arisen de novo because the variations were not detected in the parents. The BD case from the literature had not been analyzed (Kozlowski et al., 1981).

In addition, mutations in the *SOX9*, *SF1*, *DHH*, and *CBX2* genes in Case 3 were excluded as causes of XY sex reversal, as were the loss of *SRY*, del9p24.3 and the duplication of *DAX1*.

#### 4 | DISCUSSION

The POCD, an apparently underrecognized condition, was diagnosed in three hydropic fetuses and in one museum exhibit on the basis of characteristic clinical and radiological features. We identified mutations in the *FLNB* gene in POCD (Cases 1–3) as has been shown by Krakow et al. (2004) and Bicknell et al. (2005) in AO1 and BD. *FLNB* mutations

have also been shown to cause milder manifestations, such as AO3, Larsen syndrome, seemingly isolated congenital talipes equinovarus and recessive spondylocarpotarsal synostosis (Daniel et al., 2012; Krakow et al., 2004; Yang et al., 2016). However, our three fetal cases are the first cases of POCD in which *FLNB* mutations were found.

The features observed in POCD allow its classification as a distinct entity within the spectrum of giant cell osteochondrodysplasias. BD and AO1 are characterized by nonossification of all parts or of the “distal ends” of the humeri and femora, displaying a missing or seemingly global (BD) or squared and blunt (AO1) structure and associated with attenuated and shortened (in BD, bowed or boomerang like) ulnae, radii, and/or single lower leg bones, and by platyspondyly and abnormal vertebral segmentation (Farrington-Rock et al., 2006; Hunter & Carpenter, 1991; Sillence, Worthington, Dixon, Osborn, & Kozlowski, 1997). However, absolutely no ossification was found in the long tubular bones and vertebrae, excluding the lateral pedicles, of our POCD fetuses. A single cartilage anlage could be identified in the upper and lower arms and legs by direct preparation. These were short and bulky but straight and distinctly separated with missing joint formation, and the ones in the legs were in an acute angular position.

In BD and AO1, the short tubular bones have been described as very short, with predominantly the middle phalanges (BD) but in severe

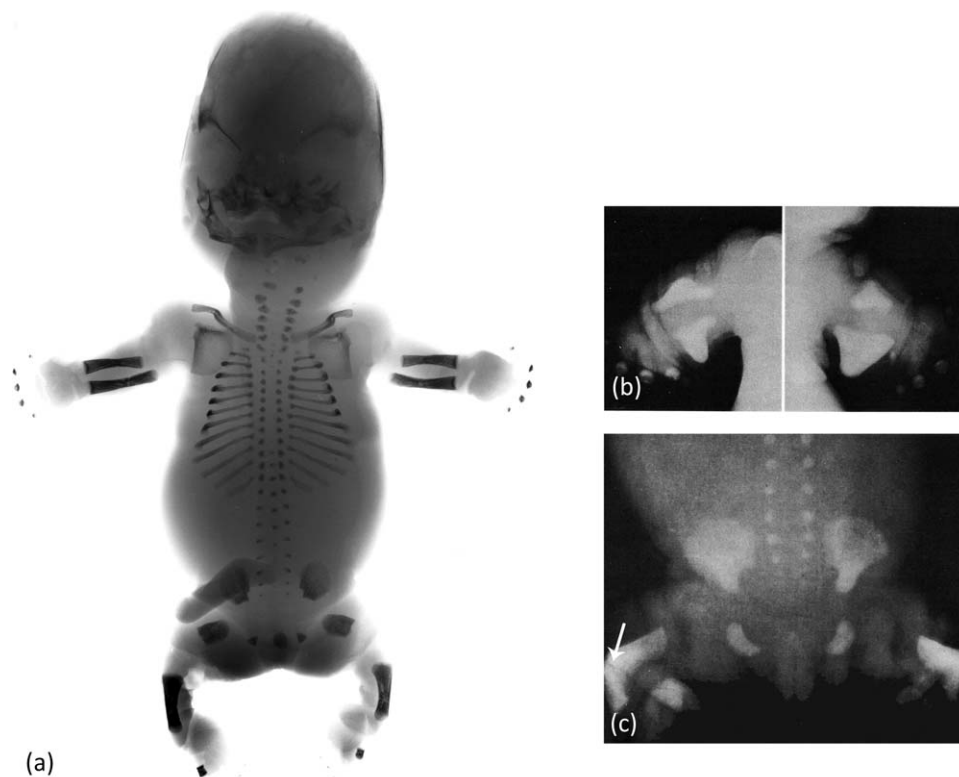


**FIGURE 5** AP fetograms of two male fetuses, one with AO1 at 16 + 2 weeks of gestation (a) and one with BD at 35 weeks of gestation (b,c). There is absent or distally lacking ossification of the humeri and femora, respectively, shortened ulnae and radii, single and shortened lower leg bones, and deficient ossification of the vertebrae and of the short tubular bones with the exception of the distal phalanges, short ribs, and small scapulae and pelvic bones—the clavicles being of almost normal size. The BD case presents with boomerang-like ulnae and radii (b), and with distinctly angulated, seemingly separated (see arrow) leg bones (c) and missing halluces (Kozłowski et al., 1981—copyright by Springer Nature)

cases also the metacarpals and proximal phalanges (AO1) unossified. Postaxial hexadactyly and partial syndactyly of the fingers have also been reported (Farrington-Rock et al., 2006; Hunter & Carpenter, 1991; Sillence et al., 1997). Again, there is absolutely no ossification of the short tubular bones in POCD fetuses. Soft tissue syndactyly of the fingers and toes is complete, leaving a thickened distal skin-covered soft tissue rim and, with regard to the rudimentary thumb in Case 3, a mitten-like hand structure. A peculiar pattern of cartilaginous finger and toe rays is revealed by cartilage staining and in histological sections. This pattern shows a missing or—in Case 3—a rudimentary thumb, a missing hallux, a missing or rudimentary first metacarpal and metatarsal, and duplication of all or of the middle and distal phalanges, resulting in distal octodactyly. While preaxial oligodactyly of the hands and feet is frequently accompanying radial and tibial defects, this special condition of preaxial oligodactyly in association with polysyndactyly and distal duplication of each of the remaining finger rays has not been previously described in AO1 or BD or in any other disorder. In addition to the duplication of the distal short tubular bones, there is segmentation of the metacarpals, giving the segments a round shape and the impression of cartilaginous pearls strung on a chain along the finger rays. These consistent findings, in addition to the flipper-like limbs and the complete failure of vertebral and tubular bone ossification, seem to be characteristic of POCD and make it possible to clearly distinguish

POCD from BD or AO1 as the most severe condition in this continuum of FLNB-related skeletal disorders. Nevertheless, there may be slight variations in the extent of nonossification concerning the lateral pedicles and ribs, as shown in Cases 1–4. There may also be overlaps with BD, as observed in the case of Urioste et al. (1997), which is equivalent to our Case 1 in the facial aspect but displays ossification of the vertebral bodies and of a single boomerang-like ossified leg bone.

In Piepkorn type of osteochondrodysplasia, the so-called giant cell chondrodysplasia is histologically characterized by monomorphic and densely packed small chondrocytes in the peripheral parts of the limb cartilage and by irregularly scattered larger chondrocytes within a homogeneous extracellular matrix in the central regions. Here, the chondrocytes present with perinuclear cytoplasmic retraction and vacuolization and with circumferential halos. The chondrocytes vary distinctly in shape and size and eventually may develop into very large cells or even into multinucleated giant cells, as shown in the POCD case of Urioste et al. (1997). However, we did not find true multinucleated giant chondrocytes in our POCD cases, except for one single giant cell-like stellate chondrocyte in Case 1, although, we recognized many giant chondrocytes in an even younger case of AO1 with the FLNB mutation localized in the CH2 region (Figure 4d).

According to the listing of 67 probands with FLNB mutations by Daniel et al. (2012), the responsible mutations in all three BD cases



analyzed (100%), in 16 of 19 AO1 cases (87%), in 6 of 13 AO3 cases (46%), and in 12 of 37 LS cases (34%) reside in exons 2 and 3 encoding CH2. CH2 represents one of the two subdomains of the ABD, which mediate and modify F-actin binding and crosslinking. As gain-of-function mutations, they have been shown responsible for giant chondrocytes, enhanced actin avidity and for filamin-actin-containing cytoplasmic focal accumulations, whose amounts correlate with disease severity (Daniel et al., 2012; Sawyer, Clark, Robertson, & Sutherland-Smith, 2009). By contrast, the heterozygous missense mutations of our three POCD fetuses were located in the immunoglobulin-like repeat 15 encoded by exons 28 and 29 of the *FLNB* gene. R15 was also the mutation site of one of the listed AO1 cases, four AO3 and five LS cases (Daniel et al., 2012; Farrington-Rock et al., 2006; Krakow et al., 2004). In fact, the only listed AO1 mutation affecting R15 presented with the same nucleotide position (c.5095), though with a different mutation type, namely a C > T transition (p.(Pro1699Ser)) in the AO1 case (Daniel et al., 2012) and a C > A transversion (p.(Pro1699Thr)) in our POCD Case 2. Mutations presenting with a same nucleotide site, but with a different amino acid exchange have already been described to cause different *FLNB*-related disorders. But identical mutations have also been reported, causing both, AO1 and AO3 (c.604A > G), AO3 and LS (c.5071G > A) or even AO1, AO3, and LS (c.502G > A) (Bicknell et al., 2005; Daniel et al., 2012; Farrington-Rock et al., 2006; Krakow et al., 2004). This could be due to the unspecificity of these *FLNB* mutations not being solely responsible for the phenotype, but needing additional genetic or epigenetic modifiers.

Since immunocytochemical examinations of cases with mutations affecting R14 and R15—including the AO1 case with the c.5095C > T mutation—did not demonstrate filamin-actin-containing focal accumulations in chondrocytes and, as shown in our cases, lack true multinucleated giant cells, the pathogenetic mechanisms resulting from these mutations are thought to differ from the gain-of-function mutations that affect CH2 (Daniel et al., 2012).

In campomelic dysplasia, XY sex reversal and skeletal dysplasia may be associated because of the regulatory function of the responsible *SOX9* gene on *COL2A1* gene expression (Bell et al., 1997). No similar functional relationship between *FLNB* and a sex-determining gene is known, and so far, sex reversal has not been observed in any of the *FLNB*-related disorders. Thus, we must assume that the association of POCD and XY sex reversal in our Case 3 is coincidental.

Our results show that the Piepkorn type of osteochondrodysplasia is a distinct clinical entity presenting with the most severe phenotype within the LS-AO3-AO1-BD-POCD continuum and is characterized by POCD-specific morphological and radiological features and by mutations in exons 28 and 29 of the *FLNB* gene, which encode the repeat region R15 of the filamin B protein. Because of the small number of POCD cases having been analyzed, this does not contradict the view, that exons encoding CH2, R14 and R15 represent hot spots for mutations that cause ossification disorders of almost identical phenotypes by different pathomechanisms (Daniel et al., 2012).

Within the setting of a new classification of skeletal dysplasias, sharing common genetic pathways, there have been efforts to reduce nosological designations, as for example, to assign the different *FLNB*-

related severe manifestations of underossification to one term, namely to AO1 (Warman et al., 2011). This may be justified from a development-oriented approach. From the perspective of prenatal diagnosticians or fetal pathologists, who are confronted with the most severe, prenatally lethal conditions of skeletal dysplasias, distinct recognizable features that can be associated with designated phenotypic pictures might be more helpful for rapid diagnostic decisions and goal directed molecular analyses. Thus BD will easily be diagnosed in the presence of boomerang-like tubular bones, AO1 in the presence of nonossification of “distal parts” of tubular bones and we hope that flipper-like limbs, complete enchondral nonossification of tubular bones and vertebrae and preaxial oligodactyly associated with polysyndactyly of each of the remaining finger rays will become keyfeatures for the diagnosis of POCD. For this reason the original terms should be maintained to enable prenatal diagnosticians to differentiate between severe skeletal dysplasias, between hydropic fetuses with cystic hygromas and to distinguish between different grades of severity within nosological entities that each are defined by a distinct phenotype.

## ACKNOWLEDGMENTS

Our thanks go to Lucia Goldhammer, Petra Krupitza (Marburg), Marion Hagl, and Britta Kluge (Vienna) for their assistance, to Prof. Matthias Meyer-Wittkopf (Oldenburg) and Astrid Becker (Leverkusen) for the contacts with the involved families and to PD Dr. Philipp Peloschek and Mrs. Bilik (Vienna) for the computer tomography and the three-dimensional reconstruction of the exhibit. We are especially indebted to Dr. Beatrix Patzak and Eduard Winter (Fool's Tower collection, Vienna), and to the Austrian Mucopolysaccharidose Society (S.G.K.) for their support. We thank Springer Nature and Edition Hausner (Vienna) for permission to reprint Figure 5b-c and Figure 1d Kozłowski et al. (1981) and Hausner (1998).

## CONFLICT OF INTEREST

All contributors declare that there is no conflict of interest.

## ORCID

Helga Rehder  <http://orcid.org/0000-0002-5215-623X>

## REFERENCES

- Bell, D. M., Leung, K. K. H., Wheatley, S. C., Ng, L. J., Zhou, S., Ling, K. W., ... Cheah, K. S. E. (1997). *SOX9* directly regulates the type-II collagen gene. *Nature Genetics*, 16(2), 174–178.
- Bicknell, L. S., Morgan, T., Bonafé, L., Wessels, M. W., Bialer, M. G., Willems, P. J., ... Robertson, S. P. (2005). Mutations in the *FLNB* cause boomerang dysplasia. *Journal of Medical Genetics*, 42(7), e43.
- Canki-Klain, N., Stanescu, V., Stanescu, R., Sinkovec, J., Debevec, M., & Maroteaux, P. (1992). Lethal short limb dwarfism with dysmorphic face, omphalocele and severe ossification defect: Piepkorn syndrome or severe “boomerang dysplasia”. *Annales De Genetique*, 35(3), 129–133.
- Chakarova, C., Wehnert, M. S., Uhl, K., Sakthivel, S., Vosberg, H.-P., van der Ven, P. F. M., & Fürst, D. O. (2000). Genomic structure and fine

- mapping of the two human filamin gene paralogues *FLNB* and *FLNC* and comparative analysis of the filamin gene family. *Human Genetics*, 107(6), 597–611.
- Cunningham, C. C., Gorlin, J. B., Kwiatkowski, D. J., Hartwig, J. H., Janmey, P. A., Byers, H. R., & Stossel, T. P. (1992). Actin-binding protein requirement for cortical stability and efficient locomotion. *Science*, 255(5042), 325–327.
- Daniel, P. B., Morgan, T., Alanay, Y., Bijlsma, E., Cho, T. J., Cole, T., ... Robertson, S. P. (2012). Disease-associated mutations in the actin-binding domain of filamin B cause cytoplasmic focal accumulations correlating with disease severity. *Human Mutation*, 33(4), 665–673.
- Farrington-Rock, C., Firestein, M. H., Bicknell, L. S., Superti-Furga, A., Bacino, C. A., Cornier-Daitre, V., ... Krakow, D. (2006). Mutations in two regions of *FLNB* result in atelosteogenesis I and III. *Human Mutation*, 27(7), 705–710.
- Hausner, E. (1998). Das pathologisch-anatomische Bundesmuseum. Edition Hausner, p51.
- Hunter, A. G. W., & Carpenter, B. F. (1991). Atelosteogenesis and boomerang dysplasia: A question of nosology. *Clinical Genetics*, 39(6), 471–480.
- Kozłowski, K., Tsuruta, T., Kameda, Y., Kan, A., & Leslie, G. L. (1981). New forms of neonatal death dwarfism. Report of 3 cases. *Pediatric Radiology*, 10(3), 155–160.
- Krakow, D., Robertson, S. P., King, L. M., Morgan, T., Sebald, E. T., Bertolotto, C., ... Cohn, D. H. (2004). Mutations in the gene encoding filamin B disrupt vertebral segmentation, joint formation and skeletogenesis. *Nature Genetics*, 36(4), 405–410.
- Nakamura, F., Stossel, T. P., & Hartwig, J. H. (2011). The filamins: Organizers of cell structure and function. *Cell Adhesion & Migration*, 5(2), 160–169.
- Oostra, R. J., Dijkstra, P. F., Baljet, B., Verbeeten, B. W. J. M., & Hennekam, R. C. M. (1999). A 100-year-old anatomical specimen presenting with boomerang-like skeletal dysplasia: Diagnostic strategies and outcome. *American Journal of Medical Genetics*, 85(2), 134–139.
- Piepkorn, M., Karp, L. E., Hickok, D., Wiegenstein, L., & Hall, J. G. (1977). A lethal neonatal dwarfing condition with short ribs, poly-syndactyly, cranial synostosis, cleft palate, cardiovascular and urogenital anomalies and severe ossification defect. *Teratology*, 16(3), 345–350.
- Sawyer, G. M., Clark, A. R., Robertson, S. P., & Sutherland-Smith, A. J. (2009). Disease-associated substitutions in the filamin B actin binding domain confer enhanced actin binding affinity in the absence of major structural disturbances: Insights from the crystal structures of filamin B actin binding domains. *Journal of Molecular Biology*, 390(5), 1030–1047.
- Schoner, K., Axt-Flidner, R., Bald, R., Fritz, B., Kohlhase, J., Kohl, T., & Rehder, H. (2017). Fetal pathology of neural tube defects—An overview of 68 cases. *Geburtshilfe und Frauenheilkunde*, 77(5), 495–507.
- Sillence, D., Worthington, S., Dixon, J., Osborn, R., & Kozłowski, K. (1997). Atelosteogenesis syndromes: A review, with comments on their pathogenesis. *Pediatric Radiology*, 27(5), 388–396.
- Stossel, T. P., Condeelis, J., Cooley, L., Hartwig, J. H., Noegel, A., Schleicher, M., & Shapiro, S. S. (2001). Filamins as integrators of cell mechanics and signalling. *Nature Reviews Molecular Cell Biology*, 2(2), 138–145.
- Superti-Furga, A., Unger, S., & Nosology Group of the International Skeletal Dysplasia Society. (2007). Nosology and classification of genetic skeletal disorders: 2006 revision. *American Journal of Medical Genetics Part A*, 143A(1), 1–18.
- Urioste, M., Rodriguez, J. I., Bofarull, J. M., Toran, N., Ferrer, C., & Villa, A. (1997). Giant cell chondrodysplasia in a male infant with clinical and radiological findings resembling the Piepkorn type of lethal osteochondrodysplasia. *American Journal of Medical Genetics*, 68(3), 342–346.
- Van der Flier, A., & Sonnenberg, A. (2001). Structural and functional aspects of filamins. *Biochimica Et Biophysica Acta*, 1538(2–3), 99–117.
- Warman, M. L., Cormier-Daire, V., Hall, C., Krakow, D., Lachman, R., LeMerrer, M., ... Superti-Furga, A. (2011). Nosology and classification of genetic skeletal disorders: 2010 revision. *American Journal of Medical Genetics Part A*, 155(5), 943–968.
- Yang, H., Zheng, Z., Cai, H., Li, H., Ye, X., Zhang, X., ... Fu, Q. (2016). Three novel missense mutations in the filamin B gene are associated with isolated congenital talipes equinovarus. *Human Genetics*, 135(10), 1181–1189.

## SUPPORTING INFORMATION

Additional Supporting Information on modified alcian blue dyeing technique may be found online in the supporting information tab for this article.

**How to cite this article:** Rehder H, Laccone F, Kircher SG, et al. Piepkorn type of osteochondrodysplasia: Defining the severe end of *FLNB*-related skeletal disorders in three fetuses and a 106-year-old exhibit. *Am J Med Genet Part A*. 2018;176A:1559–1568. <https://doi.org/10.1002/ajmg.a.38828>